

Development of the Haystack Ultrawideband Satellite Imaging Radar

Mark G. Czerwinski and Joseph M. Usoff

In February 2014, the Haystack Ultrawideband Satellite Imaging Radar joined the U.S. Space Surveillance Network as the highest-resolution space-object-imaging radar in the world. Its principal mission is to collect space-object identification and characterization data in support of space situational awareness.



The Haystack Ultrawideband Satellite Imaging Radar (HUSIR) is Lincoln Laboratory's latest iteration in the technological evolution of high-performance wideband radar systems. As is the case with HUSIR, the distinctive attribute of wideband radar is its ability to resolve a target's individual scattering centers in range, with resolution inversely proportional to bandwidth. If the radar is coherent and the pulse-repetition frequency is sufficiently high, the radar data can be processed to form inverse synthetic aperture radar (ISAR) images and high-resolution range profiles that can be used to identify and characterize targets of interest (Figure 1).

Lincoln Laboratory's history with wideband radars dates back to the 1960s, when, motivated by the need to identify and discriminate ballistic missile warheads from other objects, Lincoln Laboratory began to develop high-power wideband radar technology. The first such radar was the Advanced Research Projects Agency (ARPA)-Lincoln C-band Observables Radar (ALCOR), which became operational at Kwajalein Atoll, Marshall Islands, in 1970. With its 5.7 GHz center frequency, 0.5 GHz bandwidth, 50 cm range resolution, and 23 dB single-pulse signal-to-noise ratio (SNR) on a 1 m² target at a range of 1000 km, ALCOR pushed the envelope of then-available technology. While ALCOR was intended to support the development of discrimination techniques for ballistic missile defense, it was quickly recognized that ALCOR, among other wideband radars, could also be used to identify and characterize high-interest objects in space. The development of ISAR algorithms specifically designed for imaging space objects followed soon after [1].

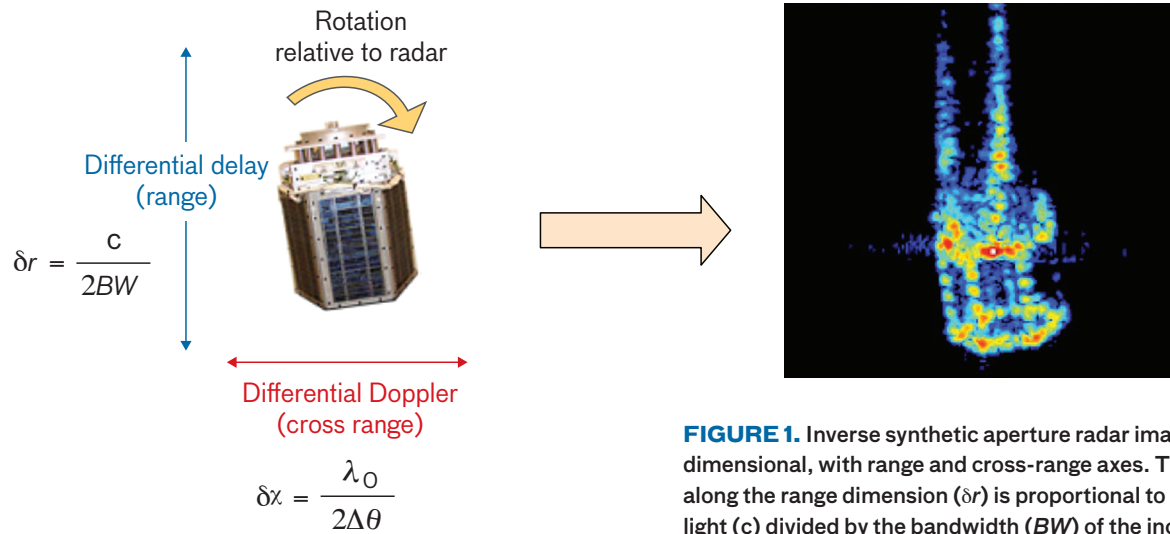


FIGURE 1. Inverse synthetic aperture radar images are two-dimensional, with range and cross-range axes. The resolution along the range dimension (δr) is proportional to the speed of light (c) divided by the bandwidth (BW) of the incident pulse. The resolution along the cross-range dimension (δx) is proportional to the wavelength (λ_0) divided by the extent of rotation of the object ($\Delta\theta$) relative to the radar.

By 1971, ALCOR images had become an indispensable operational tool for space situational awareness. ALCOR's relatively small antenna and low transmitter power limited it to imaging objects in low Earth orbit (LEO); however, its success prompted interest in extending radar imaging capabilities to targets at geosynchronous ranges and in improving image resolution. In 1978, under ARPA sponsorship, Lincoln Laboratory completed the upgrade of the 1960s Haystack radar to X band (10 GHz). The Haystack Long-Range Imaging Radar (LRIR), as it was named, had 1 GHz bandwidth, 25 cm resolution, and sufficient sensitivity to detect, track, and image satellites at geosynchronous Earth orbit (GEO) range, i.e., approximately 40,000 km (see sidebar). This effort was followed by the development of the Ka-band Millimeter-Wave (MMW) radar (initially with a 1 GHz bandwidth, which was upgraded to 2 GHz and, more recently, to 4 GHz) at Kwajalein in 1983 and the Ku-band Haystack Auxiliary (HAX) radar (2 GHz bandwidth and 13 cm range resolution) at Millstone Hill in Westford, Massachusetts, in 1993 (Figure 2).

However, by the mid-1990s, it became clear that even 13 cm resolution was insufficient for imaging a new class of small, low-cost satellites that were being built to perform sophisticated missions. Engineers at government, academic, and commercial research centers, such as the U.K.-based Surrey Satellite Technologies Ltd., were

developing microsattellites that provided high levels of capability in small packages and that were relatively inexpensive to build and much less expensive to launch than their larger counterparts [2].

Analysts examining radar images of space objects follow a rule of thumb that 20 to 30 resolution cells across an object are required to determine its shape. Even better resolution is desirable for tasks such as change detection or the determination of component function. Thus, reliably identifying and characterizing sub-meter-class objects in space would require approximately 3 cm or better range resolution (Figure 3). This resolution could be achieved by using an 8 GHz transmitter bandwidth, with further resolution improvements achieved through advanced processing techniques such as bandwidth extrapolation [3].

Usage of frequency bands in the electromagnetic spectrum is government regulated in most countries, which typically abide by international frequency allocation agreements, with the International Telecommunications Union being the predominant international spectrum management organization. In the United States, the Federal Communications Commission and the National Telecommunications and Information Administration are responsible for regulating radio-spectrum usage. The lowest frequency band that includes allocation of 8 GHz of continuous bandwidth for radar use is the

Haystack Long-Range Imaging Radar

By 1970, the Advanced Research Projects Agency (ARPA)-Lincoln C-band Observables Radar (ALCOR) had demonstrated two-dimensional imaging of low-Earth-orbit (LEO) satellites. The utility of this imaging was immediately apparent to the intelligence community; however, because of its limited sensitivity, ALCOR could only image satellites up to about 1000 km in altitude. In September 1971, two Lincoln Laboratory staff members, Gordon Guernsey and Robert Bergemann, proposed that the X-band (7.8 GHz) Haystack planetary radar may have sufficient sensitivity to detect a satellite in geosynchronous Earth orbit (GEO). An experiment conducted in September 1971 confirmed this hypothesis. Yet, the Haystack planetary radar was inherently narrowband and was only capable of imaging planet-sized objects.

The Haystack Long-Range Imaging Radar (LRIR) program (1972–1978) was intended to demonstrate that a radar with at least the bandwidth of ALCOR and at least the sensitivity of Haystack could image satellites up to GEO altitudes while significantly improving the capability to image satellites in LEO.

When completed, the Haystack LRIR was the highest-resolution and most sensitive wideband radar in the world. While the Millimeter-Wave and Haystack Auxiliary radars eventually surpassed LRIR in resolution, LRIR's capability to image satellites at geosynchronous altitudes and beyond remains unique. In addition to its role in imaging deep-space satellites, LRIR has been collecting data on LEO space-debris populations since 1990 in support of the National Aeronautics and Space Administration's Orbital Debris Program [a]. Following the 2013 upgrade to the Haystack Ultrawideband Satellite Imaging Radar, the Hay-

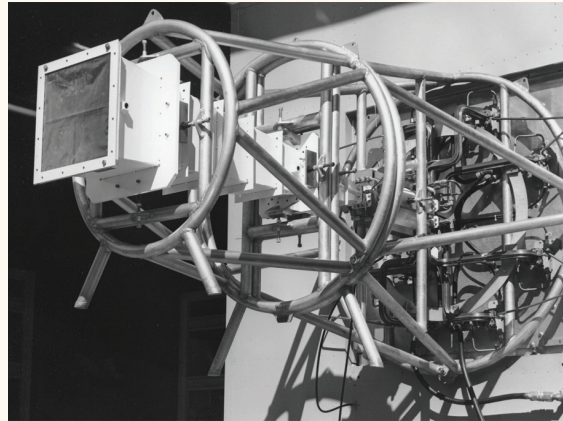


FIGURE A. The LRIR feed is integrated with the RF box prior to its insertion into the antenna. The feed and its support structure are the only components external to the RF box. Contained inside the box are the high-voltage tube stand, waveguide combiner network, and receiver hardware.

stack LRIR took on an additional role, serving as the acquisition sensor for the W-band radar.

The LRIR heavily leveraged several features of the existing Haystack facility. The Haystack antenna had excellent gain at X band, and its antenna azimuth and elevation rates were sufficient for imaging most LEO satellites. The 1 MW high-voltage power supply and capacitor bank used by the planetary radar were reused for LRIR. In addition, the ability to house the new radar equipment in the radio-frequency (RF) box that could be hoisted and plugged into the Cassegrain focus of the antenna was very attractive (Figure A).

To achieve its 400 kW peak power, LRIR combines four VTX-5681 100 kW coupled-cavity traveling-wave tubes (CC-TWTs) with 1 GHz bandwidth at 10 GHz center frequency. The tubes were developed by Varian Associates specifically for LRIR, but have since been adapted for use in several other high-power instrumentation radars [b].

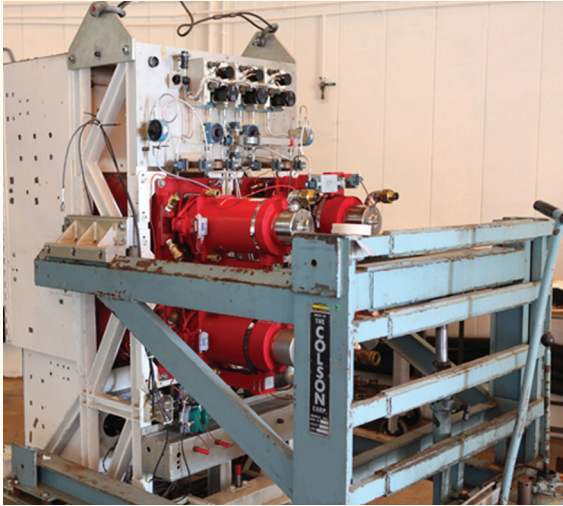


FIGURE B. On its trolley, the high-voltage tube stand is prepared for insertion into the RF box. The CC-TWTs are the red cylindrical devices protruding from the stand; the white box structure serves to protect service personnel from the high voltages used in the tube and to shield them from X rays.

For more information on TWTs, see the article “The HUSIR W-Band Transmitter” in this issue of the *Lincoln Laboratory Journal*.

The 8 × 8 × 12-foot RF box houses most of the LRIR components, including

- Four high-power CC-TWTs and a modulator
- RF driver amplifiers and their phase and gain compensation networks
- Chilled-water manifolds and control and monitoring instrumentation
- RF networks, including high-power combiners, phase-shifting networks, RF monitoring networks, and a multimode monopulse feed
- Low-noise amplifiers, a dewar, and a cryogenic pump
- High-power circulators and receiver protectors
- Downconverters, correlation mixers, intermediate frequency amplifiers, filters, and signal components
- Terminal boards and test points for all signal levels

- Test-signal injection points
- Sensors (directional couplers, arc detectors, reflected-power detectors, etc.)
- Cable trays
- Miscellaneous power supplies

The high-voltage power supply and the Radar Open Systems Architecture signal processing and control computers are located on the ground.

The design of the LRIR RF box was the result of an intricate interplay between mechanical, electrical, microwave, and human factors engineering. The RF networks, equipment, and mounts must be mechanically rugged to maintain performance when they are subjected to changing gravitational and acceleration loads and to vibrations resulting from antenna motion. The TWTs operate with 42 kV beam voltage and 10 A beam current, so high-voltage distribution and protection requirements are very complex. The box layout provides service personnel with access to the internal components and protection from high-voltage currents (Figure B).

REFERENCES

- a. G. Stansberry, M. Matney, T. Settecerri, and A. Bade, “Debris Families Observed by the Haystack Orbital Debris Radar,” *Acta Astronautica*, vol. 41, no. 1, 1997, pp. 53–56.
- b. B.G. James and L.T. Zitelli, “A 100 kW Peak 50 kW Average Coupled-Cavity TWT with 10% Bandwidth Centered at 10 GHz,” *IEEE International Electron Devices Meeting*, vol. 21, 1975, p. 133.

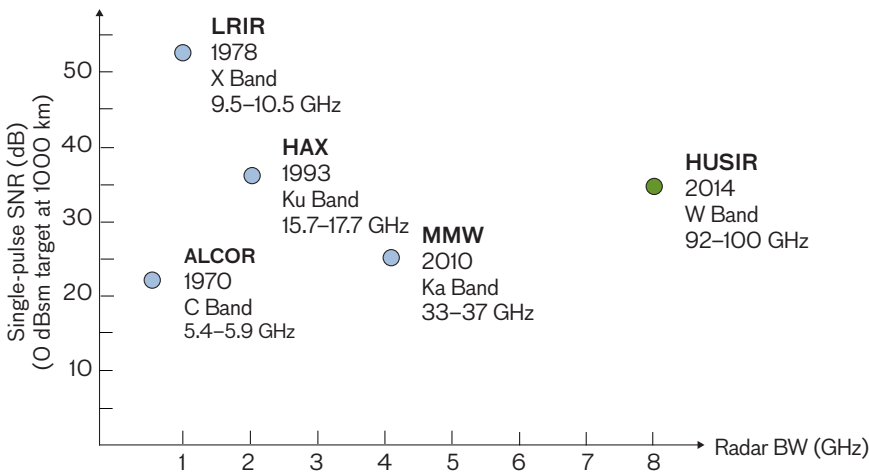


FIGURE 2. The bandwidth and resolution of space-object-imaging radars have progressed in factors of two from ALCOR to LRIR to HAX to MMW (upgraded) to HUSIR. The next step in enhancing radar performance will be to increase radar sensitivity, indicated by single-pulse signal-to-noise ratio in this figure, by increasing transmitter output power. Each of these radars operates with a bandwidth that is ~10% of its operating frequency; progression to even higher bandwidths will require higher operating frequencies.

92–100 GHz band (W band). While there are other allocated radar bands at higher frequencies that also include 8 GHz of bandwidth, the atmospheric losses at these bands are significantly higher than those at W band, and microwave components are either not available at these bands or are much more expensive than at W band. For these reasons, W band was chosen by the Lincoln Laboratory team as the desired frequency band for HUSIR; it coincides with a low-loss atmospheric absorption window that falls between the 60 GHz and 119 GHz oxygen absorption lines (Figure 4).

Antenna gain and receiver loss determine how much transmitter power is required. A high-efficiency antenna with Haystack’s 120-foot diameter could produce ~89 dB of antenna gain; cryogenically cooled wide-band low-noise amplifiers (40 K noise temperature) that were previously developed for radio astronomy could be used for the receiver. However, one concern with using a 120-foot-diameter antenna at W band was that the resulting antenna beamwidth would be very small, ~10 times smaller than the beamwidth at X band. Accordingly, the cross-sectional area of the beam used to find targets would be ~100 times smaller at W band than at X band, making initial acquisitions of targets very challenging. Even at X band, target acquisition can be difficult. In fact, the wider-beamwidth Millstone Hill radar is occasionally employed to initially find targets and help the X-band LRIR to acquire them. One way to alleviate the concern regarding antenna beamwidth would be to retain X-band LRIR capability and add W-band capability, enabling dual X- and W-band radar operation. Targets

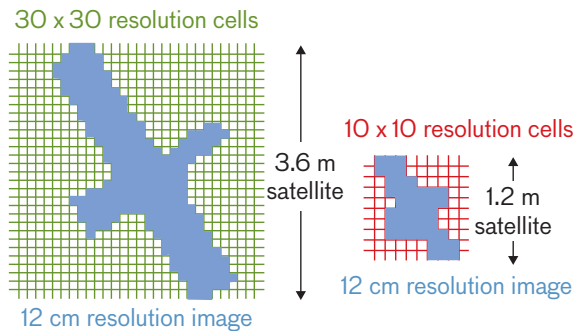


FIGURE 3. Silhouettes of a notional satellite with two solar panels are shown on pixelated grids, with pixel size corresponding to resolution. While the phenomenology and algorithms leading to ISAR image formation are very different from those depicted above, this illustration effectively shows the relationship between an object’s size and the resolution required to determine its shape.

would initially be acquired with the X-band radar and subsequently acquired with the W-band radar.

On the basis of these considerations, Lincoln Laboratory proposed adding a W-band radar at Haystack to operate simultaneously with the X-band LRIR and upgrading the 120-foot Haystack antenna with a new dish having sufficient surface accuracy to support W-band operation. Because the Haystack LRIR was the only radar in the world capable of imaging satellites at geosynchronous ranges, an important objective was to preserve its unique capabilities without degrading its preupgrade performance.

The U.S. Air Force accepted the Laboratory’s proposal and initiated the HUSIR program to image satellites in

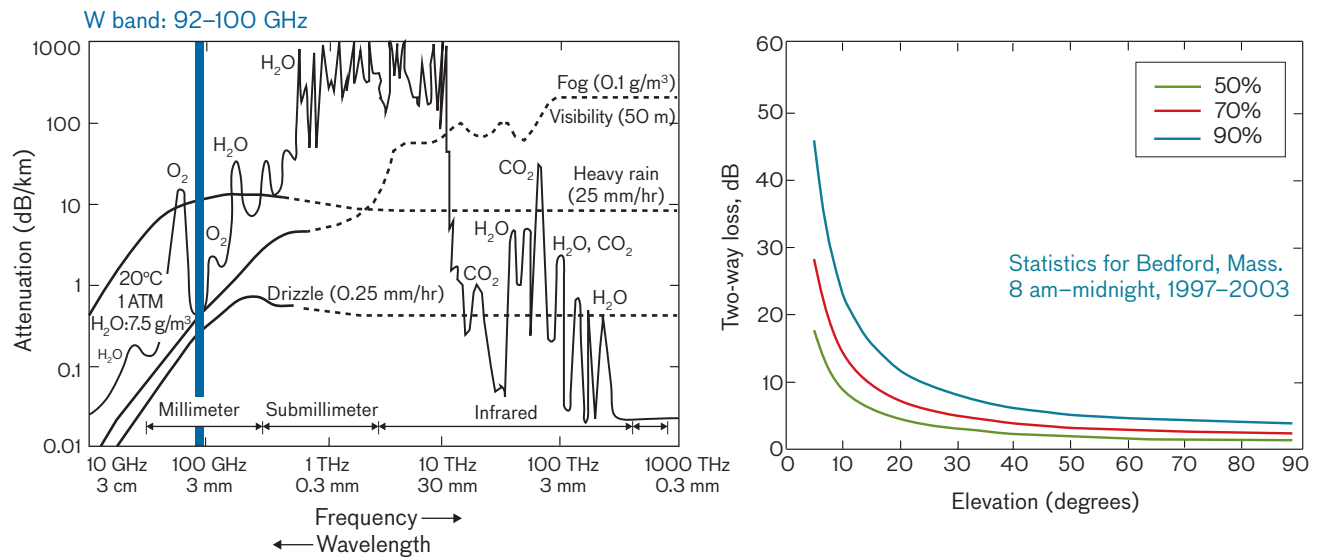


FIGURE 4. The graph on the left shows the attenuation of electromagnetic waves propagating through the atmosphere as a function of frequency [4], with W band situated in a trough between two oxygen absorption peaks; null depth between these peaks varies from day to day depending on the air's water-vapor content. The graph on the right shows attenuation (two-way loss) as a function of elevation angle. The three curves shown are based on local weather statistics, e.g., 90% of the time, the atmospheric attenuation falls below the blue curve. As the elevation approaches the horizon, the attenuation increases since the radar beam must pass through more atmosphere to reach the target. On hot humid days, operations may be constrained to elevations above 20°; on dry days, targets may be tracked down to the horizon.

LEO. Concurrently, the Defense Advanced Research Projects Agency (DARPA) funded a program to develop high-power transmitter technology that would allow HUSIR to achieve W-band sensitivity comparable to that of the X-band LRIR and enable high-resolution imaging of objects at geosynchronous range.

Transmitter

The Haystack LRIR, with a 67 dB antenna gain at X band and a transmitter combining four 100 kW coupled-cavity traveling-wave tubes (CC-TWTs), is able to track and image space objects in GEO. With the 2013 upgrade of the Haystack (subsequently referred to as HUSIR) antenna to a 100 μm root-mean-square (rms) surface tolerance, the gain at W band is 89 dB, but the atmospheric losses at W band are significantly higher. In order to achieve sensitivity similar to that of LRIR in most weather conditions, HUSIR would need a W-band transmitter with more than 100 kW of output power. A 500 W transmitter would be sufficient for tracking and imaging satellites in LEO, with sensitivity comparable to that of the HAX Ku-band radar. However, when the project was initiated, no device existed that could meet

HUSIR's bandwidth and power requirements. Gallium arsenide (GaAs) solid-state amplifiers could provide the required bandwidth, but not the required output power. Linear-beam vacuum-electron devices (e.g., CC-TWTs) have a proven track record in lower-frequency radars such as LRIR, HAX, and MMW. However, in linear-beam devices, the electron beam must be in very close proximity to the interaction circuit walls, and the wavelength is determined by the transverse circuit dimensions, typically 10% of the wavelength [5].

On the basis of these parameters, the 3 mm HUSIR wavelength would require about a 0.3 mm transverse dimension for the interaction circuit. The fabrication of devices with such small dimensions and tight tolerances is exceedingly difficult. Moreover, maintaining these tight tolerances in the presence of thermal loading resulting from electron-beam interception and RF ohmic heating is problematic. To overcome these issues at millimeter-wave frequencies, the thermonuclear fusion community pioneered the development of gyro-devices for plasma heating in tokamak reactors [6]. Electrons in gyro-devices follow helical paths around magnetic field lines and transfer energy to an electromagnetic wave by

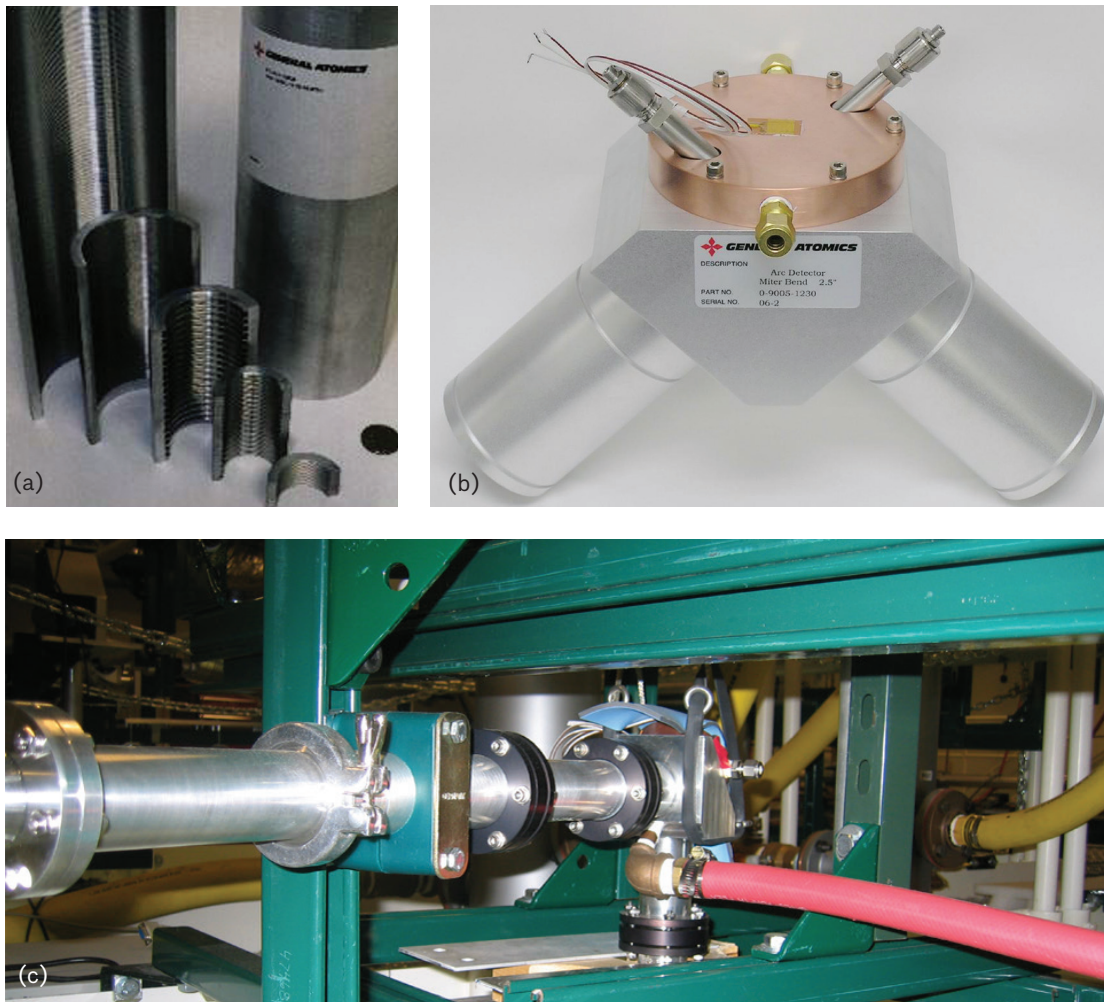


FIGURE 5. A very-low-loss overmoded waveguide is used to transfer the W-band RF energy from the transmitter to the antenna feed. Three components are shown above: (a) a waveguide section revealing interior corrugations, (b) a polarizing waveguide miter bend, and (c) a section of the installed waveguide.

means of the electron-cyclotron-resonance effect. Unlike linear-beam devices in which the wavelength is determined by the circuit dimensions, gyro-devices have a wavelength determined by the applied magnetic field strength; thus, the circuit dimensions can be significantly larger than the operating wavelength. A drawback of gyro-devices is the need for superconducting magnets to provide the high-strength magnetic fields required for high-frequency operation [7].

The potential use of gyro-devices in millimeter-wave radars was first recognized in the former Soviet Union and then at the Naval Research Laboratory (NRL), which led an effort to develop high-power wideband gyro-devices at Ka and W bands. A major challenge in realizing a wideband, high-gain, high-power gyrotron

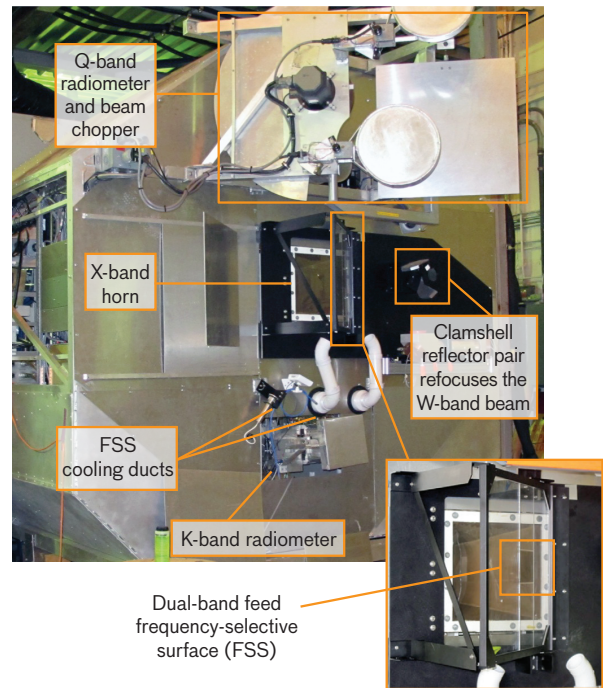
traveling-wave tube (gyro-TWT) was suppressing spurious oscillations. NRL developed a ceramic loading structure that allows the tube to operate in a higher-order mode by eliminating oscillations and demonstrated it in a 100 kW Ka-band gyro-TWT [8]. While the demonstrated bandwidth was only 1 GHz and the center frequency was 35 GHz, this success suggested that the design could be adapted to meet HUSIR requirements—an approach endorsed by leading gyrotron experts from NRL, Communications and Power Industries (CPI), and the MIT Plasma Science and Fusion Center at a gyro-TWT summit meeting held at Lincoln Laboratory on 19 February 2003. NRL agreed to select and characterize the materials for the W-band ceramic loading structure; CPI was awarded the contract to develop a 500 W, 40%-



FIGURE 6. The protruding X-band feed is clearly visible in the preupgrade LRIR RF box sitting in the special transporter (above top). An octagonal extension was added to the RF box to house the W-band radar feed, duplexer, and receiver, and radio-astronomy instrumentation—K-band, Q-band, and, in the future, W-band radiometers (right). The HUSIR RF box is shown in the transporter (above bottom).

duty gyro-TWT for HUSIR; and NASA’s Jet Propulsion Laboratory was contracted to develop the solid-state GaAs monolithic microwave integrated circuit to serve as the driver for the gyro-TWT. As built, the transmitter output power is approximately 800 W (band average), exceeding the original specification.

The complete gyro-TWT assembly with the superconducting magnet was much too large and heavy to install at the antenna near the feed. A conventional rectangular WR-10 waveguide for W-band transmission suffers about 2.6 dB per meter loss. Since the closest practical location for the transmitter equipment is about 100 m from the feed, the waveguide loss would clearly be unacceptable. Instead, a low-loss overmoded waveguide, which was also developed for plasma heating applications, is used to transfer the RF energy from the W-band transmitter to the antenna feed (Figure 5). This waveguide is 62.5 mm in diameter and operates in the HE_{11} mode, resulting in very low loss at W band. The manufacturer of the waveguide, General Atomics, specifies a loss of 0.0008 dB per meter for this size waveguide at HUSIR operating frequencies. The waveguide includes switches that allow the gyro-TWT to function as a driver for the DARPA high-power-transmitter test bed and to transmit the RF energy to the RF equipment



box on the antenna. For a more detailed explanation of HUSIR’s transmitter development, see the article “The HUSIR W-Band Transmitter” in this issue of the *Lincoln Laboratory Journal*.

Radio-Frequency Box

The original Haystack antenna was designed to accommodate interchangeable $8 \times 8 \times 12$ -foot RF equipment boxes located at the vertex of the primary reflector. Before the upgrade to HUSIR, one of these boxes was dedicated to house the LRIR X-band transmitter, the feed, and the front-end receiver. When the Haystack antenna was configured to be used as a radio telescope, another box, housing the astronomy radiometers, was installed. Changing the mode from radio telescope to radar required a series of steps: (1) the astronomy RF box was disconnected and lowered to the ground; (2) the LRIR RF box housing the X-band transmitter, the feed, and the receiver was hoisted 80 feet up into the antenna; (3) all cables and hoses were connected, and the system was checked out. This process typically took at least one full eight-hour shift. To support the dual use of the antenna, the LRIR RF box was modified to accommodate the radio-astronomy radiometers and feeds, and the W-band waveguide, receivers, and the X and W dual-band feed (Figure 6). The switchover

from radar to radio-astronomy mode can now be accomplished in minutes. The antenna continues to be available to Haystack Observatory for radio astronomy and other scientific research on a noninterference basis as per an agreement with the U.S. Air Force.

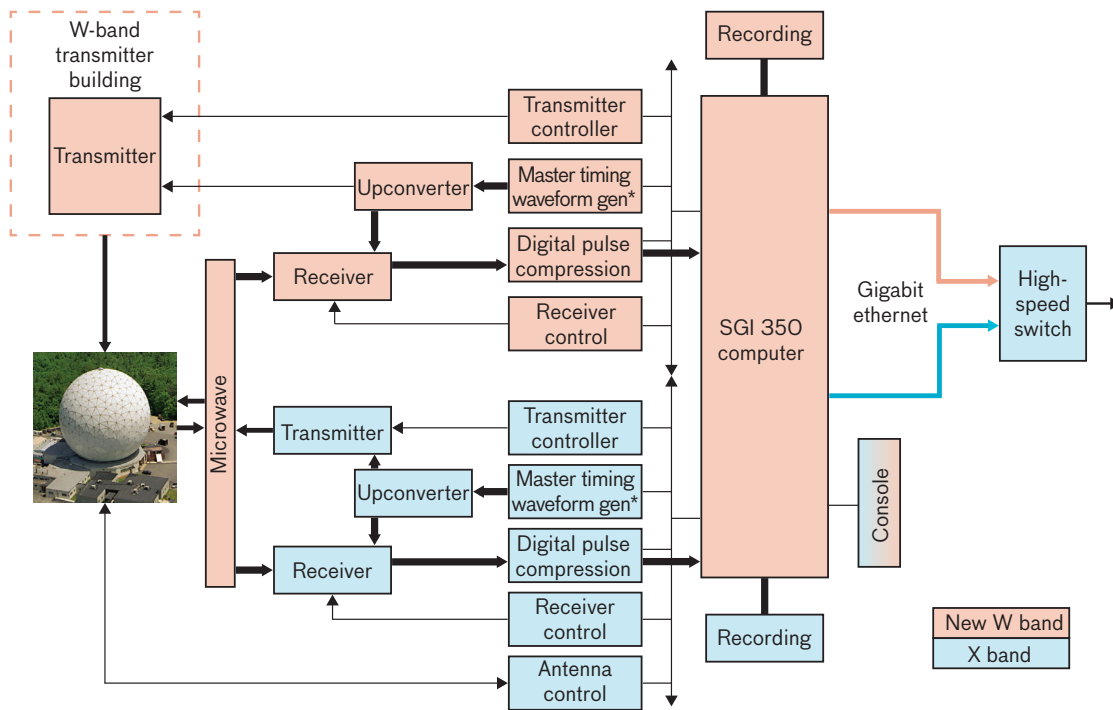
Processing and Control

The HUSIR dual-band feed allows X-band and W-band beams to be co-boresighted and both radars to operate simultaneously. In typical operations, X- and W-band trackers run concurrently, but only one tracker, designated “prime,” is used to close the tracking loop. Initially, the X-band tracker is prime and is used for early target acquisition and tracking. When the precision track is established, the W-band tracker becomes prime. Once the target is in track at W band, target signature data are simultaneously collected in both bands.

The processing and control hardware and software for HUSIR are based on the Lincoln Laboratory Radar Open Systems Architecture (ROSA) that is used on the

other Lincoln Space Surveillance Complex radars in Westford, Massachusetts, and on the radars at the Reagan Test Site on Kwajalein Atoll [9]. Because ROSA already included support for dual-band radars, almost all of the approximately 500,000 lines of code (for the real-time program [RTP], displays, and support software) were reused. Only about 5% of the RTP software needed to be modified or replaced for HUSIR, including the X-band to W-band tracking transition. The ROSA simulator allowed testing and debugging of the RTP modifications early in the program, and, remarkably, almost no software issues were encountered during the integration and test phases.

A block diagram of the HUSIR-ROSA signal processing system is shown in Figure 7. The W-band system is subdivided into functional building blocks in a manner identical to the X-band system. Each autonomously developed building block or subsystem follows a well-defined interface so that it may be incorporated into the complete system. Commercial off-the-shelf (COTS) equipment is used as much as possible, but some new



*gen = generator

FIGURE 7. In this block diagram of the HUSIR-ROSA signal processing system, blue blocks represent preupgrade X-band system components; orange blocks represent components that had to be added or replaced to support W-band capability.

development was required. For example, the waveform generator was designed and built at Lincoln Laboratory because no COTS equipment met all of the requirements for this component.

One signal processing challenge that needed to be addressed was the effect of tropospheric scintillation on W-band coherence. Radio astronomers have observed that the coherence time at 3 mm wavelength is largely limited by phase noise resulting from fluctuations in total path delay through the troposphere. Since RF propagation through the troposphere is approximately nondispersive (i.e., the delay does not strongly depend on the wavelength), this effect is much less noticeable at longer wavelengths. Because pulse-to-pulse coherence measured to within a fraction of a wavelength is critical to forming focused ISAR images, tropospheric scintillation needs to be corrected. Measurements of the phase variation were conducted during the early stages of the program, and autofocus algorithms that use radar data to determine and remove this random phase variation were developed. By applying these algorithms, focused images were generated immediately at the beginning of the full-bandwidth W-band testing; only relatively modest refinements were needed to improve data quality. For more details, see the article “HUSIR Signal Processing” in this issue.

Antenna

When the original 120-foot Haystack Cassegrain antenna was completed in 1964 with 1 mm (1000 μm) rms surface tolerance, it provided excellent performance in the 8–10 GHz frequency range and was considered an engineering marvel. To achieve comparable aperture efficiency at W band, the rms surface departure from a perfect paraboloid would need to be about 0.1 mm (100 μm)—the width of a human hair or a sheet of 20-pound copy paper (Figure 8). A few radio-telescope antennas comparable in size and surface tolerance to HUSIR have been built. However, unlike these purely scientific research instruments, the HUSIR antenna would need to maintain this accuracy while tracking LEO satellites at relatively high angular rates and with elevation-related gravity effects over a full range of diurnal temperature variations.

One option considered at the conceptual design phase was an actively controlled deformable primary reflector surface segmented into hexagonal panels, each supported by three actuators, with a closed-loop interferometric laser

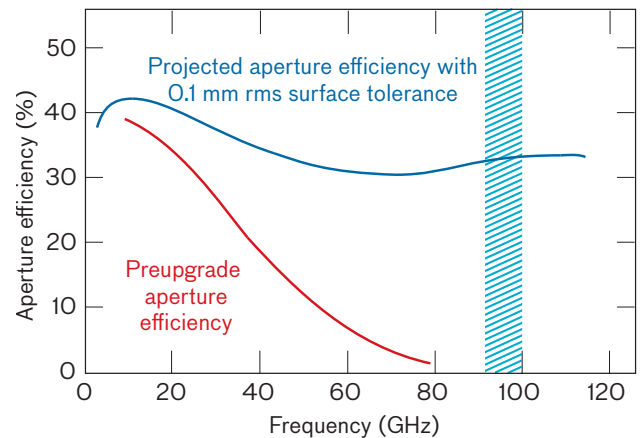


FIGURE 8. The aperture efficiency, including radome losses, of the original antenna dropped off at W band (92–110 GHz) as a result of manufacturing tolerance deviations and gravity and thermal deformations of the reflector surface panels. The projected aperture efficiency shown above is based on the original radome membrane; however, during the upgrade, this membrane was replaced with a new material optimized for W band. With this new membrane, the actual aperture efficiency in W band is better than 40%.

measurement system to compensate for gravitational and thermal distortions. This concept produced several concerns: the design would be very complex, the real-time measurement and control system needed to adjust the surface would introduce significant risk, and the continual maintenance required by the actuators would reduce the operational availability of the antenna. However, a preliminary structural design for the antenna, developed by Simpson Gumpertz & Heger Inc. (SGH) of Waltham, Massachusetts, suggested that the HUSIR specifications could be met with a relatively lightweight but stiff aluminum-welded antenna backstructure and a steel transition structure, supported by the legacy Haystack pedestal and yoke. The SGH design allows the primary reflector structure to deform under the influence of gravity and temperature gradients without losing its approximately parabolic surface; only the focal length is affected. To compensate for the focal-length changes, the position of the rigid aluminum secondary subreflector is continuously adjusted with changing elevation. A more detailed summary of the antenna design concepts may be found in Antebi and Kan [10].

The structural design of the antenna proved to be sound although much more difficult to fabricate to the required tolerances than originally anticipated. The assembly toler-

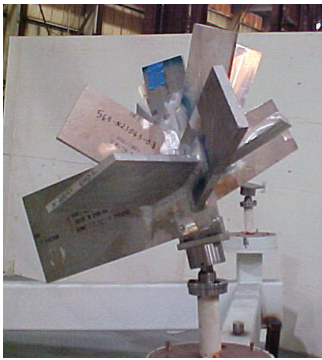


FIGURE 9. The special jigs that Ranor Corporation devised were used to weld nodes (above) and ribs in assembly fixtures (right).



ance budget for the 120-foot aluminum-welded backstructure was 0.34 inches. The backstructure is a space truss of 6061-T6 aluminum tubes of various diameters optimized to be lightweight and stiff. The nodes at which the tubes join together are exceedingly complex; a typical node joins between 10 and 15 tubes uniting at various angles specified within half a degree of precision. Welding a large aluminum structure while maintaining this level of precision was no easy feat. Skilled welders at Ranor Corporation of Westminister, Massachusetts, devised special jigs for holding components in place while the largest subassemblies that could be trucked to the Haystack site were welded (Figure 9). To provide a suitable sheltered environment for completing the welding of the backstructure, a 140 × 160-foot temporary building was erected at the site (Figure 10).

Installation of the antenna was planned to minimize the amount of downtime for the Haystack LRIR. Major antenna components, including the backstructure, quadrapod, and the transition structure, were completed at the Haystack site while the radar was still operating. Once the components of the new antenna were complete, the radome was split in two and the 141-foot-diameter, 115,000-pound radome cap was removed and set aside. The old antenna was removed in large pieces and reduced to scrap. The yoke was then modified to accept the new antenna, and the radome cap was reskinned with a new membrane that has lower transmission loss at W band and improved hydrophobicity compared to the old membrane. When the yoke modifications were completed, the new 155,000-pound transition structure was installed, followed by the installation of the new backstructure and quadrapod. Finally, the

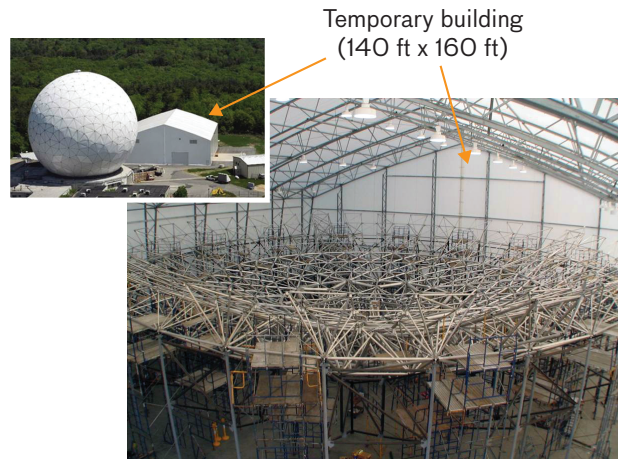


FIGURE 10. A temporary building at the Haystack site offered a low-wind environment suitable for welding the backstructure assembly.

radome cap was replaced. Only after the remainder of the radome membranes were replaced were the 104 surface panel assemblies installed on the backstructure. The panels were manufactured to a 28 μm rms tolerance, and great care was taken to avoid exposing them to the environment or damaging them during transport or handling. Following initial alignment of the reflector surface panels, the subreflector was installed.

Removal of the old antenna structure, fabrication of the new major assemblies, and installation of the new antenna required careful planning and clever use of the limited space that is available near the Haystack facility (Figure 11).

The disassembly of the old antenna and the installation of the new one entailed heavy construction work requiring the use of a large-capacity (750 ton) crane, supplied by

Assembly sequence

1. Erect assembly building
2. Assemble backstructure
3. Assemble transition structure
4. Prepare site for construction
5. Install crane
6. Remove radome cap
7. Remove old antenna
8. Modify yoke
9. Assemble quadrapod
10. Remove assembly building
11. Install transition structure
12. Attach quadrapod to backstructure
13. Install backstructure
14. Replace radome cap
15. Remove crane
16. Restore site
17. Install subframes

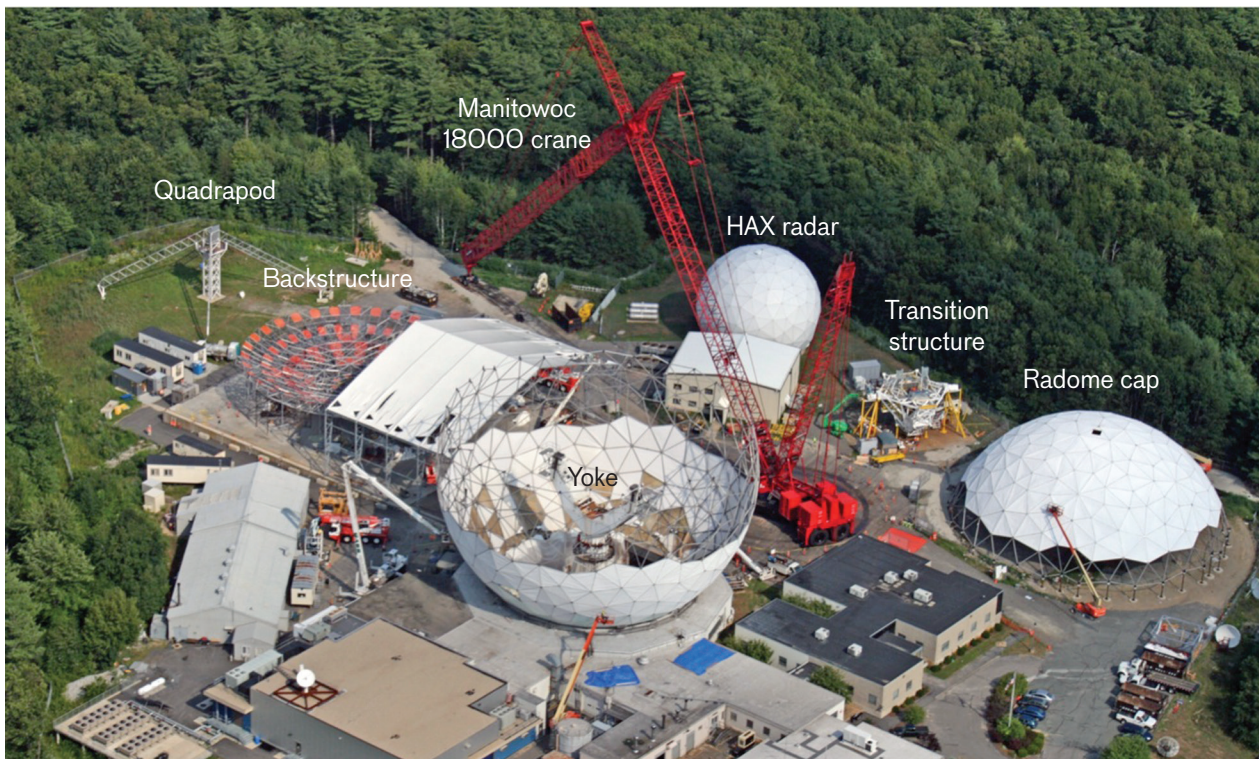
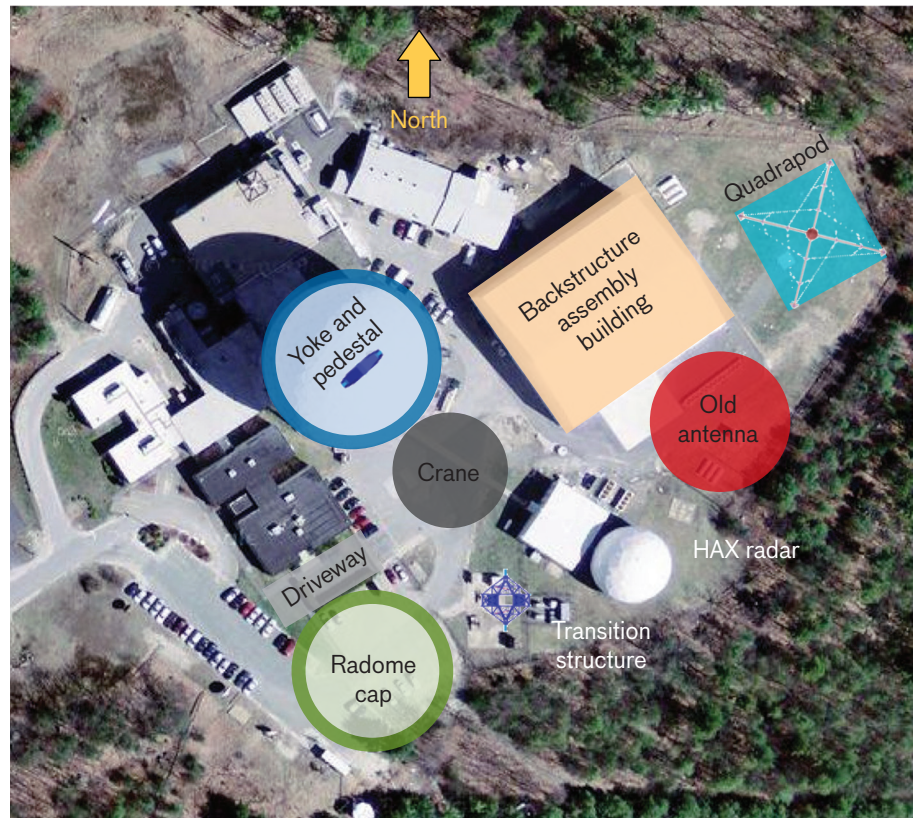


FIGURE 11. Aerial photographs of the Haystack site were taken before the installation process began (above top) and during the antenna construction when the backstructure assembly building was in the process of being removed and the radome cap had been reskinned (above bottom).

Hallamore Corporation of Holbrook, Massachusetts, and a skilled ironworker team, assembled by Keystone Engineering, formerly of Georgetown, Massachusetts. Bond Brothers of Everett, Massachusetts, was awarded the contract for construction and site safety management, which was critical throughout the disassembly and installation process. Because the risk of damage to the antenna was very real, each lift was backed by rigorous engineering analysis and detailed procedures and drawings. Lincoln Laboratory staff members and the ironworker team worked closely together to ensure that the antenna was assembled with the required precision and handled with care to avoid damage. The entire installation—from taking the radome cap off to putting it back on—was completed in summer 2010 without any mishaps. For more details on the installation, see the article “Construction of the HUSIR Antenna” in this issue.

One of the design goals for the original Haystack antenna had been to maintain smooth and precise tracking at very slow rates, a capability that requires minimum stiction (static friction). To minimize stiction, the antenna yoke was rotated about the azimuth axis on an externally pressurized oil-film hydrostatic bearing [11]. The nominal thickness of the oil film was only 0.004 inches. The new antenna, as designed, would be heavier than the original antenna. As built, it is even heavier than designed; the weight on the azimuth bearing is 50% greater than that of the original. Although the hydrostatic bearing was upgraded to provide additional oil flow to maintain the film thickness, it seized up during control system testing. After extensive testing, measurements, and analysis, it was discovered that the bearing surfaces deform when a significant difference exists between the bearing oil temperature and the yoke temperature. Under some conditions, this difference could lead to loss of film thickness and to metal-to-metal contact. To correct the distortion, additional stiffeners were added to the bearing structure, the hydraulic system was upgraded to lower the oil temperature and increase film thickness, and an instrumentation system was developed to measure film thickness in real time and stop the antenna if the film’s thickness decreased below a preset threshold.

Surface Alignment

As they were installed, the surface panel assemblies were aligned to a theoretical paraboloid with approximately 2 mm rms surface tolerance by using laser trackers. Once all of the subframes were installed, a second

round of subframe alignment was conducted using a laser radar (ladar) that was mounted in place of the sub-reflector at the quadrapod apex. The ladar method was sufficiently accurate to achieve satisfactory alignment for X-band radar operation; however, this method proved to be insufficient to achieve the 100 μm tolerances required for W band. A third round of alignment was conducted by applying a microwave holography technique. Using the signal emitted by a K-band Internet service provider on a geosynchronous satellite, this technique involves mapping out the far-field antenna pattern by scanning the HUSIR antenna. Because the signal is not time coherent, a small 7.9-foot-diameter reference antenna is used to measure the phase. The complex far-field antenna pattern is then transformed into a two-dimensional map of the antenna surface; this map is used to compute the number of turns needed for each of the 416 screws employed to adjust the surface. After the adjustments are made, the measurement process is repeated until the process converges. For HUSIR, it took 13 iterations to achieve the measured surface tolerance of approximately 75 μm rms (the error model predicts that even under worst-case thermal conditions, the surface error should remain under 105 μm rms). Details of the alignment process are provided in the article “Optimizing the HUSIR Antenna Surface” in this issue.

Integration and Testing

The W-band transmitter and the signal processing subsystems were completed before the installation of the new antenna. In order to verify their functionality and performance, they were integrated with the same small 7.9-foot reflector antenna that was subsequently used for holography measurements. The small antenna, which was equipped with a controller identical to the one used on the large 120-foot reflector, was placed on the roof of the transmitter facility, hence the name Rooftop Radar (Figure 12). The Rooftop Radar was initially used to collect data on a corner reflector located 42 km away on Mount Pack Monadnock in southern New Hampshire. At this range and essentially 0° elevation, the tropospheric attenuation is approximately 15 times greater than the tropospheric attenuation at zenith. This test provided a good opportunity to validate the sensitivity model and verify the system’s phase stability and coherence (Figure 13). Because of its low gain, the rooftop antenna could not

track any satellites except the International Space Station (ISS); nonetheless, its ability to track and image the ISS in W band proved that the radar transmitter and signal processing operated correctly, eliminating much of the risk associated with full system integration.

After the initial surface alignment and antenna integration, the top priority was to restore the X-band LRIR to operation. All LRIR functions were checked out, and tests were conducted to verify that the performance was not degraded relative to the preupgrade baseline. The

LRIR integration and testing (I&T) were conducted concurrently with the holography surface alignment and the data collection for the precision mount model (0.001° absolute pointing accuracy) required for W-band operation. After X-band performance was verified, the LRIR became available for tasking by operational users, while I&T of the W-band radar system continued until 5 November 2013. In February 2014, after successful completion of the Air Force Space Command operational trial period, HUSIR became a contributing sensor to the U.S. Space Surveillance Network (Figures 14 and 15).

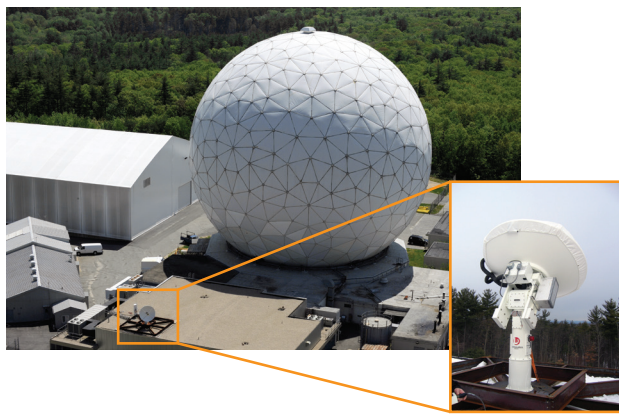


FIGURE 12. The 7.9-foot rooftop antenna was used for initial integration and testing before the 120-foot antenna was completed.

Performance

The principal goal of the HUSIR program—to demonstrate unprecedented image quality for timely on-demand identification and characterization of objects in space—was achieved. While radar images of space objects remain classified, Figure 16 illustrates the difference in ISAR image quality between 1 GHz and 8 GHz radar bandwidths. In addition to resolution improvements achieved with the greater bandwidth, scattering from small features is enhanced at shorter wavelengths. With a W-band antenna gain of 89 dB, HUSIR achieves higher single-

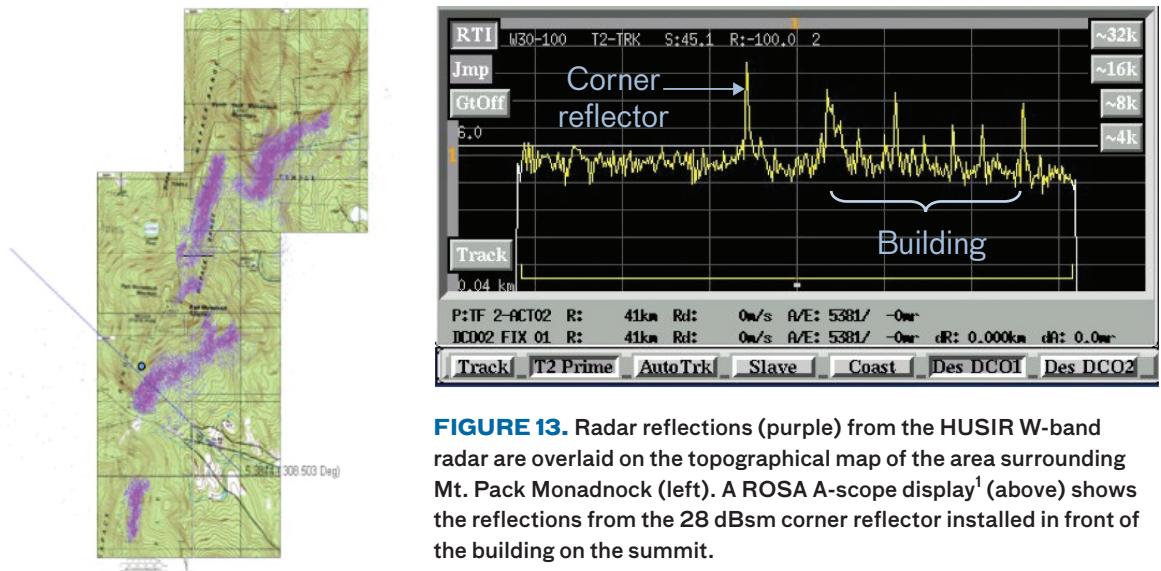


FIGURE 13. Radar reflections (purple) from the HUSIR W-band radar are overlaid on the topographical map of the area surrounding Mt. Pack Monadnock (left). A ROSA A-scope display¹ (above) shows the reflections from the 28 dBsm corner reflector installed in front of the building on the summit.

¹ An A-scope display shows the amplitude of reflected radar energy as a function of range.

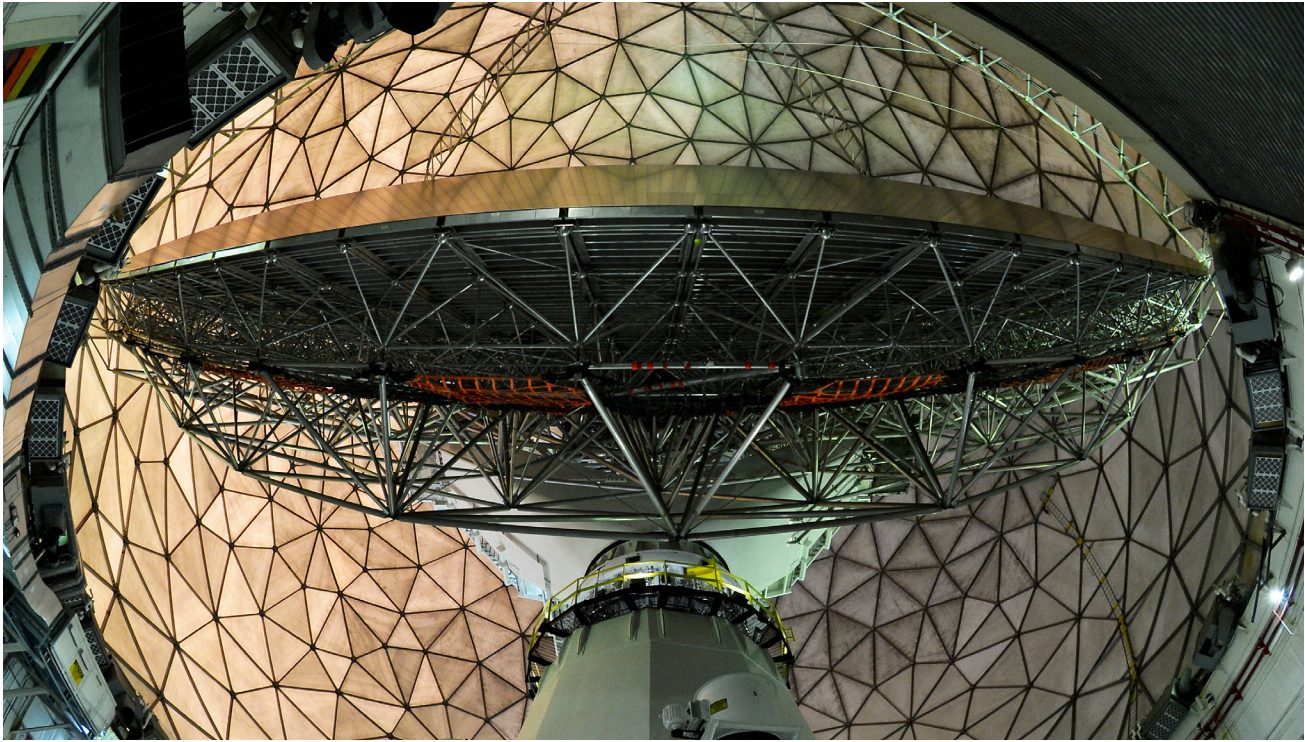


FIGURE 14. Only a few inches of clearance exist between the edges of the reflector and the space frame of the radome; as a result, the photographer resorted to a fisheye lens to capture the completed HUSIR antenna in its entirety, as shown above. The photograph was taken during a ribbon-cutting ceremony held on 11 February 2014 at the Lincoln Space Surveillance Complex to welcome HUSIR to the U.S. Space Surveillance Network.



FIGURE 15. (Left to right) Lt Gen Ellen M. Pawlikowski, Commander, Space and Missile Systems Center, Air Force Space Command; Gen William L. Shelton, Commander, Air Force Space Command; and Dr. Eric D. Evans, Director, Lincoln Laboratory, perform the honors at HUSIR's ribbon-cutting ceremony.

pulse sensitivity than HAX, despite using only 800 W of transmitter power (compared to 100 kW for HAX).

Future Directions

HUSIR is currently the highest-resolution space-object-imaging radar in the world. Even before integration and testing phases were completed, HUSIR data helped to identify and characterize high-interest objects in space. Now, as a contributing sensor to the U.S. Space Surveillance Network, HUSIR continues to play a key role in LEO space situational awareness. With a W-band antenna gain of 89 dB and the application of the high-power transmitter technology demonstrated under the DARPA program, HUSIR could match the sensitivity of the X-band LRIR and attain high-resolution identification and characterization of satellites in the geosynchronous orbit regime.

A critically important role for HUSIR is to serve as a test bed for new technologies and operational concepts. New capabilities such as real-time imaging would enable the identification of small satellites within tactical time-

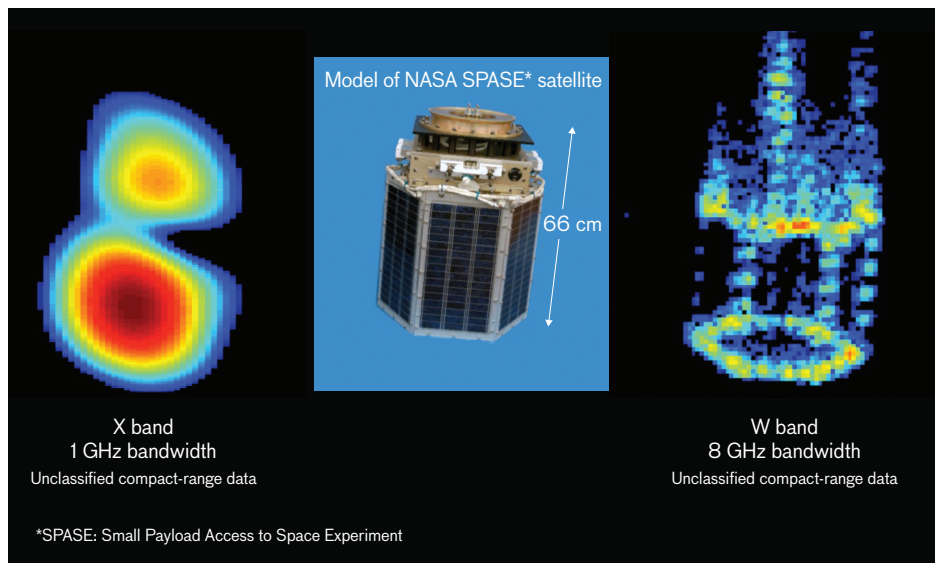


FIGURE 16. Unclassified compact-range imagery data of a NASA Small Payload Access to Space Experiment (SPASE) satellite model has been processed to depict the difference in resolution between 1 GHz and 8 GHz radar bandwidths.

lines. Recent advances in gallium nitride (GaN) power amplifiers at W-band frequencies open up the possibility of replacing the current vacuum-tube transmitter with a solid-state transmitter to improve reliability and frequency response and potentially lower life-cycle costs.

In addition to the X- and W-band radars, the HUSIR antenna also accommodates science instruments. With a $100\ \mu\text{m}$ rms surface, the antenna will have good aperture efficiency in frequencies up to the 230 GHz band, making HUSIR a premier instrument for millimeter-wave radio astronomy. For example, the ability to observe methanol and silicon-monoxide masers at high frequencies could provide new insights into the physics of early low-mass star formation and the atmospheres of dying stars. In addition to supporting single-dish radio-astronomy research, Haystack will become a pivotal site in the very-long-baseline interferometry global network of antennas and the Event Horizon Telescope network of radio telescopes, with the goal of imaging the environment surrounding the supermassive black hole at the center of our galaxy [12]. Haystack will also continue to be utilized in radio-astronomy educational programs for students. For more information on HUSIR's applications to astronomy, see the article "Insights into the Universe: Astronomy with Haystack's Radio Telescope" in this issue.

For years to come, HUSIR will provide operational support to the space situational awareness mission, to the development and demonstration of technology for

national security, and to world-class scientific research and education.

Acknowledgments

The initial work on HUSIR was jointly sponsored by the Air Force Electronic Systems Center (ESC) and the DARPA Tactical Technology Office. Antenna development and system integration and testing were sponsored by the Space Command and Control and Surveillance Division of ESC, which was later consolidated into the Air Force Life Cycle Management Center. Operational testing of HUSIR was sponsored by the Air Force Space Command. ■

REFERENCES

1. W.W. Camp, J.T. Mayhan, and R.M. O'Donnell, "Wideband Radar for Ballistic Missile Defense and Range-Doppler Imaging of Satellites," *Lincoln Laboratory Journal*, vol. 12, no. 2, 2000, pp. 267–279.
2. Surrey Satellite Technology Ltd., "Changing the Economics of Space for 25 Years," *SSTL 25 Years Brochure*, Guildford, U.K.: Surrey Satellite Technology Ltd., 2010, available online at <http://www.sstl.co.uk>.
3. S.L. Borison, S.B. Bowling, and K.M. Cuomo, "Super-Resolution Methods for Wideband Radar," *Lincoln Laboratory Journal*, vol. 5, no. 3, 1992, pp. 441–461.
4. G. Brooker, M. Bishop, and S. Scheduling, "Millimetre Waves for Robotics," *Proceedings of the Australian Conference on Robotics and Automation*, 2001, pp. 91–97.
5. M. Blank et al., "Development and Demonstration of High Average Power W-Band Gyro-Amplifiers for Radar Applications," *IEEE Transactions on Plasma Science*, vol. 30, no. 3, 2002, pp. 865–875.

6. V.L. Granatstein, B. Levush, B.G. Danly, and R.K. Parker, "A Quarter Century of Gyrotron Research and Development," *IEEE Transactions on Plasma Science*, vol. 25, no. 6, 1997, pp. 1322–1335.
7. K.L. Felch, B.G. Danly, H.R. Jory, K.E. Kreischer, W. Lawson, B. Levush, and R.J. Temkin, "Characteristics and Applications of Fast-Wave Gyrodevices," *Proceedings of the IEEE*, vol. 87, no. 5, 1999, pp. 752–781.
8. M. Garven, J.P. Calame, B.G. Danly, K.T. Nguyen, B. Levush, F.N. Wood, and D.E. Pershing, "A Gyrotron-Traveling-Wave Tube Amplifier Experiment with a Ceramic Loaded Interaction Region," *IEEE Transactions on Plasma Science*, vol. 30, no. 3, 2002, pp. 885–893.
9. S. Rejto, "Radar Open Systems Architecture and Applications," *The Record of the IEEE 2000 International Radar Conference*, 2000, pp. 654–659.
10. J. Antebi and F.W. Kan, "Replacement of Elevation Structure to Upgrade Haystack 37-m Radio Telescope," *Proceedings of SPIE, Astronomical Structures and Mechanisms Technology*, vol. 5495, 2004, pp. 137–146.
11. G.R. Carroll, "A Hydrostatic Bearing for Haystack," *American Society of Mechanical Engineers Winter Meeting*, 1962, paper no. 62-WA-299.
12. S.S. Doeleman et al., "Event-Horizon-Scale Structure in the Supermassive Black Hole Candidate at the Galactic Centre," *Nature*, vol. 455, no. 7209, 2008, pp. 78–80.



Joseph M. Usoff is a senior staff member in the Aerospace Sensor Technology Group. Since joining Lincoln Laboratory in 1993, he has performed missile seeker testing, developed an automated radar cross section diagnostic tool for stealth aircraft, developed and implemented real-time radar imaging algorithms, and, most recently, contributed to the Haystack

Ultrawideband Satellite Imaging Radar project. Prior to his Laboratory career, he worked at Raytheon as an antenna engineer, at the U.S. Air Force Radar Target Scatter Facility (RATSCAT) as the chief data analyst, and at The Ohio State University ElectroScience Laboratory as a graduate researcher. He earned a bachelor's degree in electrical engineering from Carnegie Mellon University and master's and doctoral degrees in electrical engineering from The Ohio State University.

ABOUT THE AUTHORS



Mark G. Czerwinski is the leader of Lincoln Laboratory's Aerospace Sensor Technology Group, which focuses on developing novel RF sensors and techniques, principally for space situational awareness and space control applications. He joined Lincoln Laboratory in 1978 as a staff member in the Surveillance Techniques Group, where he worked on

tracking and signal processing algorithms for the Millstone Hill radar, techniques for new launch acquisition and custody, and the development of the Space-Based Visible Processing, Operations, and Control Center. In the mid-1990s, he participated in several studies and reviews in support of the National Weather Service Modernization Program. In 1995, he became the leader of the former Radar Imaging Techniques Group, later renamed to the Imaging and Assessment Technology Group (and now called the Space Situational Awareness Group). During this time, he developed systems and techniques for space-object characterization, space mission assessment, and space situational awareness. In 2007, he became the Lincoln Laboratory program manager for HUSIR. He received a bachelor's degree from MIT and a doctoral degree from Carnegie Mellon University, both in electrical engineering.